JOURNAL OF SOLID STATE CHEMISTRY **123,** 186–189 (1996)
ARTICLE NO. 0167

LETTER TO THE EDITOR

Temperature Dependent Structural Behavior of Sr_2RhO_4

T. Vogt

Department of Physics, Brookhaven National Laboratory, Upton, New York 11973

and

D. J. Buttrey

Department of Chemical Engineering, University of Delaware, Newark, Delaware 19716

Communicated by J. M. Honig, February 20, 1996; accepted February 21, 1996

Variations in the structure of Sr_2RhO_4 as a function of temperature have been investigated using high-resolution neutron powder diffraction. The K_2NiF_4-type structure possesses microdomains distinguished by clockwise versus anticlockwise rotation of the RhO_6 octahedra. These domains have nonequivalent sizes which vary with temperature.

The occurrence of superconductivity in cuprates crystallizing with the K_2NiF_4 structure is still far from being understood. The recent discovery of superconductivity ($T_C \sim 1$ K) in Sr_2RuO_4 (1), a K_2NiF_4 structure containing a $4d^4$ transition metal with spin state $S = 1$, prompted the question of whether superconductivity could also be observed in the isostructural compound Sr_2RhO_4 where rhodium (a $4d^5$ transition metal) has a spin of $S = \frac{1}{2}$. Maeno *et al.* could not find any indication for superconductivity down to 50 mK (1). We showed that in the case of Sr_2RuO_4, in contrast with the isostructural copper-containing compounds, the onset of superconductivity is not accompanied by long-range structural distortions (2). We detected an enhanced D_{4h} distortion within the RuO_6 octahedra as a structural response to a metal-to-insulator transition near 100 K. The intriguing differences in the low temperature conductivity of the isostructural compounds Sr_2RuO_4 and Sr_2RhO_4 prompted us to investigate the temperature-dependent structural behavior of the latter compound. We believe that any theory which attempts to explain superconductivity in copper oxides must provide a framework that can be expanded to all and especially to isostructural oxides.

A 5.5 g Sr_2RhO_4 powder specimen was prepared from Johnson–Matthey Grade 1 $SrCO_3$ and Aldrich 99.8% Rh_2O_3. The starting mixture was first fired in 1 bar oxygen at 1000°C for several hours, then at 1150°C for 7 h, and finally at 1260°C for 50 h with one interruption for regrinding. It was then annealed in stages under 1 bar oxygen, ending with 5 days at 750°C, followed by furnace cooling to room temperature. The glossy black crystallites appear homogeneous with an average diameter of about 5 μm. The neutron powder diffraction experiments were performed on the high-resolution neutron powder diffractometer (HRNPD) at the High Flux Beam Reactor at Brookhaven National Laboratory. The instrumental resolution is $\Delta d/d \sim 5 \times 10^{-4}$ at a wavelength of 1.8857 Å. The instrument features a unique vertically focusing monochromator made of Ge(115) wafer stacks, where each wafer was individually deformed to obtain a highly reproducible anisotropic mosaic which provides a symmetrical peak shape at optimum resolution and flux (3, 4). The data were collected using a detector bank comprising 64 ^{3}He detectors separated by 2.5° in 2θ and stepped with 0.05°. The Rietveld refinements were done using PROFIL written by J. K. Cockcroft (University of Birbeck, UK). The sample was held in a vanadium container and placed into a high-temperature displex (Air Products). The accessible temperature range was 10–450 K. One additional measurement was done in a two-stage displex (Air Products) which can reach 3.8 K.

As revealed by the room temperature X-ray diffraction study of Itoh *et al.* (5), Sr_2RhO_4 crystallizes in a $\sqrt{2}a \times 2c$ superstructure of the parent K_2NiF_4 cell. All reflections could be indexed using this cell and the space group $I4_1/acd$. We used the same model, allowing for uncorrelated octahedral rotations about the **c**-axis, that Huang *et al.* (6) used in their refinement of Sr_2IrO_4. No extra reflections or indications of peak splitting were observed on cooling. All diffraction patterns were refined using the same crystal-

0022-4596/96 $18.00

TABLE 1
Parameters for the Sr_2RhO_4 Structure at Various Temperatures

Site	x	y	z	B	N
		T = 450 K			
		a = 5.4548(2) Å, c = 25.7522(9) Å			
Sr	0	0	0.1762(2)	0.83(9)	16
Rh	0	0	0	0.5(1)	8
O(1A)	0.2043(7)	0.2043(7)	¼	0.4(2)	14.1(2)
O(1B)	0.2957(7)	0.2957(7)	¼	0.4(2)	1.9(2)
O(2B)	0	0	0.0806(2)	0.7(1)	16
	R_{wp} = 14.7%	R_I = 9.7%	R_{exp} = 6.0%		
		T = 400 K			
		a = 5.4523(1) Å, c = 25.7571(7) Å			
Sr	0	0	0.1760(1)	0.71(8)	16
Rh	0	0	0	0.4(1)	8
O(1A)	0.2051(6)	0.2051(6)	¼	0.5(1)	14.5(2)
O(1B)	0.2949(6)	0.2949(6)	¼	0.5(1)	1.5(2)
O(2B)	0	0	0.0802(1)	0.65(8)	16
	R_{wp} = 13.9%	R_I = 8.8%	R_{exp} = 5.5%		
		T = 350 K			
		a = 5.4539(1) Å, c = 25.7579(7) Å			
Sr	0	0	0.1759(1)	0.66(8)	16
Rh	0	0	0	0.4(1)	8
O(1A)	0.2057(6)	0.2057(6)	¼	0.5(1)	15.0(2)
O(1B)	0.2943(6)	0.2943(6)	¼	0.5(1)	1.0(2)
O(2B)	0	0	0.0801(1)	0.67(9)	16
	R_{wp} = 15.8%	R_I = 7.9%	R_{exp} = 5.8%		
		T = 300 K			
		a = 5.4504(1) Å, c = 25.7606(7) Å			
Sr	0	0	0.1760(1)	0.66(8)	16
Rh	0	0	0	0.4(1)	8
O(1A)	0.2048(6)	0.2048(6)	¼	0.5(1)	15.1(2)
O(1B)	0.2952(6)	0.2952(6)	¼	0.5(1)	0.9(2)
O(2B)	0	0	0.0801(1)	0.64(9)	16
	R_{wp} = 16.3%	R_I = 7.2%	R_{exp} = 5.9%		
		T = 250 K			
		a = 5.44569(9) Å, c = 25.7654(6) Å			
Sr	0	0	0.17582(9)	0.43(6)	16
Rh	0	0	0	0.02(1)	8
O(1A)	0.2044(5)	0.2044(5)	¼	0.3(1)	15.3(1)
O(1B)	0.2956(5)	0.2956(5)	¼	0.3(1)	0.7(1)
O(2B)	0	0	0.0801(1)	0.47(7)	16
	R_{wp} = 16.8%	R_I = 9.1%	R_{exp} = 5.6%		
		T = 200 K			
		a = 5.44335(9) Å, c = 25.7676(6) Å			
Sr	0	0	0.17587(9)	0.53(6)	16
Rh	0	0	0	0.05(8)	8
O(1A)	0.2040(4)	0.2040(4)	¼	0.5(1)	15.1(1)
O(1B)	0.2960(4)	0.2960(4)	¼	0.5(1)	0.9(1)
O(2B)	0	0	0.0801(1)	0.52(7)	16
	R_{wp} = 16.2%	R_I = 8.5%	R_{exp} = 5.3%		
		T = 150 K			
		a = 5.44147(9) Å, c = 25.7714(6) Å			
Sr	0	0	0.17579(9)	0.43(7)	16
Rh	0	0	0	0.07(8)	8
O(1A)	0.2037(4)	0.2037(4)	¼	0.3(1)	15.0(1)
O(1B)	0.2963(4)	0.2963(4)	¼	0.3(1)	1.0(1)
O(2B)	0	0	0.802(1)	0.41(7)	16
	R_{wp} = 16.6%	R_I = 8.9%	R_{exp} = 5.4%		
		T = 100 K			
		a = 5.43953(8) Å, c = 25.7740(5) Å			
Sr	0	0	0.17574(8)	0.33(6)	16
Rh	0	0	0	0.16(7)	8
O(1A)	0.2036(4)	0.2036(4)	¼	0.44(9)	14.9(1)
O(1B)	0.2964(4)	0.2964(4)	¼	0.44(9)	1.1(1)
O(2B)	0	0	0.0800(1)	0.43(6)	16
	R_{wp} = 14.3%	R_I = 6.8%	R_{exp} = 5.0%		
		T = 50 K			
		a = 5.43811(9) Å, c = 25.7755(6) Å			
Sr	0	0	0.17576(9)	0.27(6)	16
Rh	0	0	0	0.00(8)	8
O(1A)	0.2031(4)	0.2031(4)	¼	0.3(1)	15.0(1)
O(1B)	0.2969(4)	0.2969(4)	¼	0.3(1)	1.0(1)
O(2B)	0	0	0.0801(1)	0.41(7)	16
	R_{wp} = 15.5%	R_I = 6.8%	R_{exp} = 5.5%		
		T = 10 K			
		a = 5.43593(9) Å, c = 25.7786(5) Å			
Sr	0	0	0.17580(8)	0.19(6)	16
Rh	0	0	0	0.02(8)	8
O(1A)	0.2027(4)	0.2027(4)	¼	0.32(9)	15.0(1)
O(1B)	0.2973(4)	0.2973(4)	¼	0.32(9)	1.0(1)
O(2B)	0	0	0.0800(1)	0.34(6)	16
	R_{wp} = 14.7%	R_I = 7.9%	R_{exp} = 5.0%		
		T = 3.8 K			
		a = 5.43562(9) Å, c = 25.7749(6) Å			
Sr	0	0	0.17591(9)	0.19(6)	16
Rh	0	0	0	0.00(8)	8
O(1A)	0.2025(4)	0.2025(4)	¼	0.2(1)	15.0(1)
O(1B)	0.2975(4)	0.2975(4)	¼	0.2(1)	1.0(1)
O(2B)	0	0	0.0803(1)	0.26(7)	16
	R_{wp} = 15.7%	R_I = 7.8%	R_{exp} = 5.2%		

lographic model. The results of these refinements are presented in Table 1. In contrast to what we have observed in Sr_2RuO_4, the unit cell shows a different response to cooling. The **a**-axis contracts in a similar manner to that observed in Sr_2RuO_4; however, the **c**-axis expands on cooling (Fig. 1). The **a**-parameter is roughly twice the in-plane Rh–O bond length. However, the lattice contraction along **a** by roughly 0.35% coincides with contraction of the in-plane Rh–O distance by only 0.2%. It is interesting that while the apical Rh–O distance contracts by 0.26%, the **c**-axis actually expands by 0.08%. As pointed out by Itoh *et*

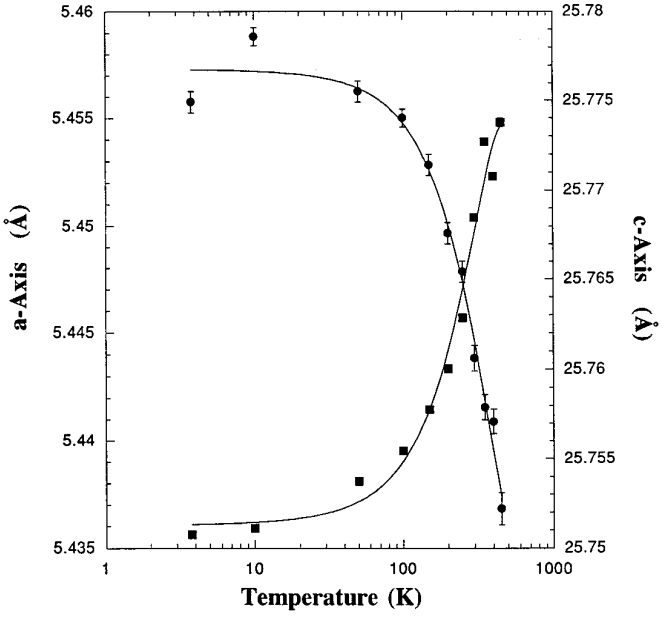

FIG. 1. Lattice constants of Sr_2RhO_4 as a function of temperature.

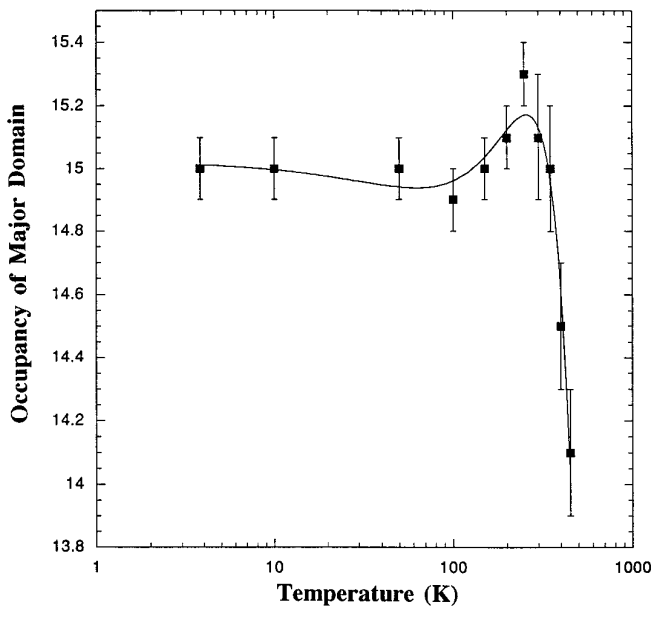

FIG. 3. The temperature dependence of the occupancy of O(1A) at $(x, x, \frac{1}{4})$ with $x \approx 0.205$, representing the majority microdomain in Sr_2RhO_4. The full site occupancy is 16.

al. (5), Sr_2RhO_4 reveals partial disordered rotations of the RhO_6 octahedra with respect to the **c**-axis. This tilt angle increases on cooling by about 3% (Fig. 2). Subramanian *et al.* (6) report a tilt angle of 9.7° at 300 K and of 10.5° at 13 K. These angles differ somewhat from our corresponding values of 10.25° at room temperature and 10.7° at 10 K. Similarly, Huang *et al.* (7) found that the tilt angle also increases by roughly 3% for Sr_2IrO_4 between room temperature and 10 K.

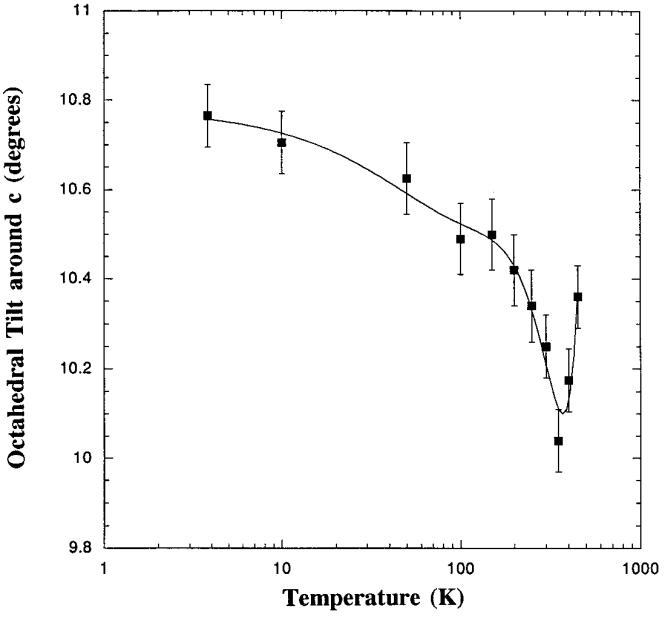

FIG. 2. Temperature dependence of tilt angles for the RhO_6 octahedra about the **c**-axis in degrees.

The unequal occupancies of the two sets of $(x, x, \frac{1}{4})$ positions indicate that the 4_1 symmetry is not consistently obeyed between neighboring RhO_2 layers along **c**. This corresponds to describing the structure as being built of short-range domains. The fact that one orientation is dominant points to disorder which could be influenced by kinetic factors associated with time and temperature during synthesis and cooling. This may explain the difference in the tilt angles observed by Subramanian *et al.* (6) and by us. The correlated thermal evolution of the tilt angle and domain occupancy shows remarkably different behavior above and below room temperature. The tilt of the RhO_6 octahedra around **c** initially decreases and then increases again below 300 K (Fig. 2). The occupancy of the major tilt domain corresponds to the occupancy of O1A (at $(x, x, \frac{1}{4})$ with $x < \frac{1}{4}$) which represents a counterclockwise tilt of the RhO_6 octahedra around the **c**-axis (Fig. 3). This major domain grows from being present at about an 88% level at $T = 450$ K to about a 95% level at 250 K and then saturates at lower temperatures.

In Sr_2MO_4 compounds with the K_2NiF_4 structure the Sr–O distance should ideally be $\sqrt{2}$ larger than the M–O distance. Deviation of the tolerance factor $t = (r_{Sr} + r_O)/\sqrt{2}(r_M + r_O)$ from unity reveals the extent of geometrical mismatch. For $t < 1$ the M–O planes are under compression and the Sr–O bonds are under tension. A structure will attempt to compensate for this strain by distorting.

One possibility is a D_{4h} octahedral distortion as is the case in Sr_2RuO_4. Alternatively, phase separation creating oxygen-rich and -deficient phases (e.g., $La_2NiO_{4+\delta}$), tetragonal-to-orthorhombic distortion, or a T-to-T′ transition (e.g., $La_{2-x}Nd_xCuO_4$) can also reduce the strain associated with mismatch. The tilting of rigid RhO_6 octahedra as observed in Sr_2RhO_4 is yet another mechanism for relieving the compressive stress felt by the RhO_2 layers due to the tensional strain occurring in the SrO layer. There are numerous studies dealing with the structural coherence of the CuO_2 planes in hole-doped copper oxide superconductors (e.g., (8) and references therein). Using high-q neutron powder diffraction data and analyzing the pair distribution functions Egami *et al*. (9) showed that, despite the fact that the high-temperature structure is tetragonal (implying no tilt angle), the local structure is actually orthorhombic. It is only when the structural coherence length approaches unit cell dimensions that the structure becomes completely incoherent with random atomic displacements and is tetragonal on average. Jorgensen *et al*. [8] proposed that the structural coherence of the CuO_2 planes is a requirement for superconductivity in layered copper oxides. With the emphasis being on coherent or incoherent rather than orthorhombic or tetragonal this conjecture may help to explain why Sr_2RuO_4 is superconducting whereas Sr_2RhO_4 is not. Assuming that the superconductivity in Sr_2RuO_4 is more BCS-like, the associated correlation length would be much larger than that of the cuprates ($\leq$30 Å) (10). It is intriguing to speculate that the absence of superconductivity in Sr_2RhO_4 may be at least partly due to the presence of microdomains on a scale which is too small to permit a sufficient correlation length for the onset of superconductivity.

ACKNOWLEDGMENT

This research was supported in part by the Division of Materials Sciences, U.S. Department of Energy, under Contract DE-AC02-76CH00016.

REFERENCES

1. Y. Maeno, H. Hashimoto, K. Yoshida, S. Nishizaki, T. Fujita, J. G. Bednorz, and F. Lichtenberg, *Nature* **372,** 532 (1994).
2. T. Vogt and D. J. Buttrey, *Phys. Rev B* **52**(14), R9843 (1995).
3. T. Vogt, L. Passell, S. Cheung, and J. D. Axe. *Nucl. Instrum. Methods A* **338,** 71 (1994).
4. J. D. Axe, S. Cheung, D. E. Cox, L. Passell, T. Vogt, and S. Bar-Ziv, *J. Neutron Res.* **2**(3), 85 (1994).
5. M. Itch, T. Shimura, Y. Inaguma, and Y. Morij, *J. Solid State Chem.* **118,** 206 (1995).
6. M. A. Subramanian, M. K. Crawford, R. L. Harlow, T. Ami, J. A. Femandez-Baca, Z. R. Wang, and D. C. Johnston, *Physica C* **235–240,** 743 (1994).
7. Q. Huang, J. L. Soubeyroux, O. Chmaissem, I. Natali Sora, A. Lantoro, R. J. Cava, J. J. Krajewski, and W. F. Peck Jr., *J. Solid State Chem.* **112,** 255 (1994).
8. J. D. Jorgensen, D. G. Hinks, B. A. Hunter, R. L. Hitterinan, A. W. Mitchell, P. G. Radaelli, B. Dabrowski, J. L. Wagner, H. Takahashi, and E. C. Larson, *in* ''Proceedings of a Workshop Held in Santa Fe, New Mexico,'' p. 85. World Scientific, Singapore, 1992.
9. S. J. L. Billinge and T. Egami, *in* ''Proceedings of a Workshop Held in Santa Fe, New Mexico,'' p. 93. World Scientific, Singapore, 1992.
10. M. Suzuki and M. Hikata, *Jpn. J. Appl. Phys.* **28,** 1368 (1989).